MULTIPHOTON EFFECTS IN CHANNELING RADIATION

M.V. Bondarenco

NSC Kharkov Institute of Physics & Technology,
Kharkov, Ukraine

October 6, 2014, Channeling-2014, Capri, Italy

Outline

Multiphoton spectrum

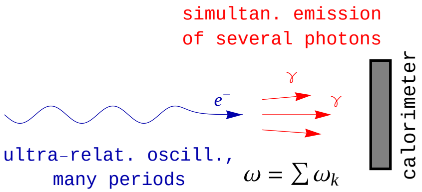

An intensely radiating ultra-relativistic electron may emit several photons in a narrow cone, and at calorimetric detection, only their total energy is measured.

$$\frac{dw}{d\omega} = \frac{1}{N_{\text{events}}} \frac{\Delta N_{\text{events}}(\sum_k \omega_k = \omega)}{\Delta\omega} \neq \frac{dw_1}{d\omega_1}$$

Single-photon spectrum $\frac{dw_1}{d\omega_1}$ is more directly related to predictions of classical electrodynamics ($\frac{dw_1}{d\omega_1} = \frac{1}{\omega_1}\frac{dI}{d\omega_1}$), whereas the multiphoton spectrum (radiative energy loss) $\frac{dw}{d\omega}$ is usually measured at practice.

Examples – spectra not proportional to the target thickness:

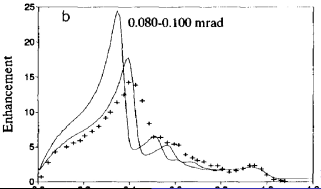

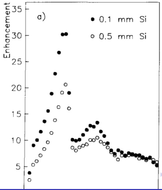

Photon multiplicity spectrum

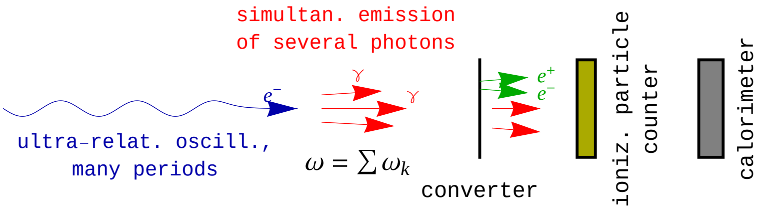

$\bar{n}(\omega)$ – mean number of photons per electron with a total radiative loss ω.
Unlike $\frac{dw}{d\omega}$, it does not vanish at large ω.

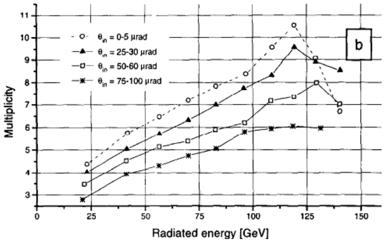

Multiphoton spectrum – equations

If single-photon spectrum $\frac{dw_1}{d\omega_1}$ is known, n-photon emission probabilities factorize and can be resummed as

$$\begin{aligned}\frac{dw}{d\omega} &= W_0 \sum_{n=1}^{\infty} \frac{1}{n!} \int_0^{\infty} d\omega_1 \frac{dw_1}{d\omega_1} \cdots \int_0^{\infty} d\omega_n \frac{dw_1}{d\omega_n} \delta\left(\omega - \sum_{k=1}^{n} \omega_k\right) \quad (1a)\\ &= e^{-\int_0^\infty d\omega_1 \frac{dw_1}{d\omega_1}} \frac{1}{2\pi i} \int_{c-i\infty}^{c+i\infty} ds e^{s\omega} \left(e^{\int_0^\infty d\omega_1 \frac{dw_1}{d\omega_1} e^{-s\omega_1}} - 1 \right), \quad (1b)\end{aligned}$$

where $W_0 = 1 - \int_0^\infty d\omega \frac{dw}{d\omega} = e^{-\int_0^\infty d\omega_1 \frac{dw_1}{d\omega_1}}$ is the photon *non*-emission probability.

The distribution function for the radiating electrons differs by a singularity:

$$\Pi(E_e - \omega) = \frac{dw}{d\omega} + W_0 \delta(\omega).$$

It is normalized to unity: $\int_0^{E_e} \Pi(E_e - \omega) = 1$, and obeys a linear kinetic equation

$$\frac{\partial}{\partial L} \Pi(E_e - \omega) = \int_0^E d\omega_1 \frac{\partial}{\partial L} \frac{dw_1}{d\omega_1} \left[\Pi(E_e - \omega - \omega_1) - \Pi(E_e - \omega) \right], \quad (2)$$

with the singular initial condition

$$\Pi(E_e - \omega)\big|_{L=0} \equiv \delta(\omega). \quad (3)$$

Possibility for reconstruction

$$\frac{dw_1}{d\omega_1} = \frac{1}{2\pi i}\int_{c-i\infty}^{c+i\infty} ds e^{s\omega_1} \ln\left(1 + W_0^{-1}\int_0^{E_e} d\omega \frac{dw}{d\omega} e^{-s\omega}\right). \quad (4)$$

E.g., if one adopts a parameterization for the multiphoton spectrum

$$\omega\frac{dw}{d\omega} = A\omega e^{-\alpha\omega}, \quad (5)$$

the reconstruction formula gives a closed-form result

$$\omega_1\frac{dw_1}{d\omega_1} = e^{-\alpha\omega_1} - e^{-\frac{\alpha}{1-A/\alpha}\omega_1}, \qquad \alpha^{-1} \ll E_e. \quad (6)$$

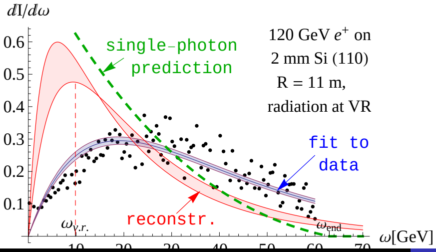

Figure: Spectrum of radiation at volume reflection. Points, data of [D. Lietti *et al.*, *NIM B* **283** (2012) 84] for StR11 crystal. Blue band, fit of (5) to experimental data, the adjusted parameter values being $A = 0.042 \pm 0.003$, $\alpha = 0.053 \pm 0.002$. Red band, reconstructed single-photon spectrum (6). Dashed green curve, prediction for the single-photon spectrum of coherent bremsstrahlung in a bent crystal [M.V. Bondarenco, *Phys. Rev. A* **81** (2010) 052903]

The photon multiplicity spectrum – equations

For the corresponding photon multiplicity spectrum, the resummation procedure yields

$$\bar{n}(\omega)\frac{dw}{d\omega} = W_0 \sum_{n=1}^{\infty} \frac{n}{n!} \int_0^{\infty} d\omega_1 \frac{dw_1}{d\omega_1} \ldots \int_0^{\infty} d\omega_n \frac{dw_1}{d\omega_n} \delta\left(\omega - \sum_{k=1}^{n} \omega_k\right) \quad (7a)$$

$$= \frac{1}{2\pi i} \int_{c-i\infty}^{c+i\infty} dse^{s\omega + \int_0^{\infty} d\omega_1 \frac{dw_1}{d\omega_1}\left(e^{-s\omega_1}-1\right)} \int_0^{\infty} d\omega_1' \frac{dw_1}{d\omega_1'} e^{-s\omega_1'}. \quad (7b)$$

It obeys $\bar{n}(0) = 1$, $\bar{n}(\omega) \geq 1$.

In case if $\frac{dw}{d\omega}$ is obtained from solving a kinetic equation, $\bar{n}(\omega)$ can be readily inferred from the differential relation

$$\bar{n}(\omega) = w_1 + L\frac{\partial}{\partial L} \ln \frac{dw}{d\omega}, \qquad w_1 = \int_0^{\infty} d\omega_1 \frac{dw_1}{d\omega_1}. \quad (8)$$

(If $\frac{dw_1}{d\omega_1} \propto L$, with L the target thickness.)

Manifestation of multiphoton effects in pure coherent radiation spectra

$$\frac{dw_{1c}}{d\omega_1} = b\left(1 - 2\frac{\omega_1}{\omega_0} + 2\frac{\omega_1^2}{\omega_0^2}\right)\theta(\omega_0 - \omega_1)$$ ('one-point' dipole spectrum).

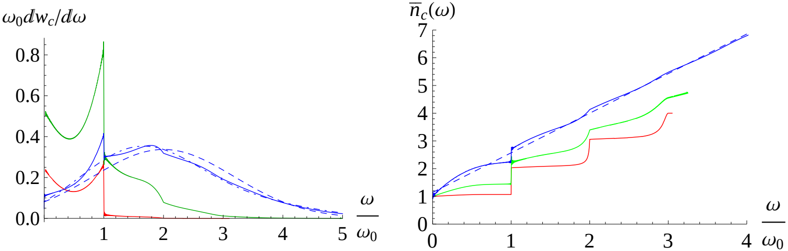

Figure: Red curve corresponds to intensity parameter $b\omega_0 = 0.3$, $\bar{n} = \frac{2}{3}b\omega_0 = 0.2$ [small deviations from the single-photon spectrum]. Green curve, the same for $b\omega_0 = 2$ (the highest summit reached by the fundamental maximum). Blue curves, $b\omega_0 = 6$ (onset of high-intensity regime). Dashed blue curve, Gaussian approximation (9). Dot-dashed blue curve, corrected Gaussian approximation (10).

- Mimicking the second harmonic
- Suppression of discontinuities
- Suppression of the low-ω region

High intensity (photon multiplicity) limit – equations

At high radiation intensity, contour integral (1) approximately evaluates by the steepest descent method, giving a Gaussian form for the multiphoton spectrum:

$$\frac{dw_c}{d\omega} \simeq \frac{e^{-\rho^2/2}}{\sqrt{2\pi\overline{\omega^2_{1\,c}}}}, \tag{9}$$

with $\rho = \frac{\omega - \overline{\omega_{1c}}}{\sqrt{\overline{\omega^2_{1\,c}}}}$ the scaling variable.

The next-to-leading order (Chebyshev) correction reads

$$\frac{dw_c}{d\omega} \simeq \frac{e^{-\rho^2/2}}{\sqrt{2\pi\overline{\omega^2_{1\,c}}}} \left[1 + \frac{\gamma_3}{12\sqrt{2}} H_3\left(\frac{\rho}{\sqrt{2}}\right)\right], \tag{10}$$

where $\gamma_3 = \frac{\overline{(\omega - \overline{\omega})^3}}{\overline{(\omega - \overline{\omega})^2}^{3/2}} = \frac{\overline{\omega_1^3}}{\overline{\omega_1^2}^{3/2}} \propto \frac{1}{\sqrt{\bar{n}}}$, and

$H_3(z) = -e^{z^2} \frac{d^3}{dz^3} e^{-z^2} = 8z^3 - 12z$ is the Hermite polynomial of order 3.
It mildly breaks the Gaussian scaling, and accounts for the residual spectral skewness.

The limiting photon multiplicity spectrum is linear: $\bar{n}_c(\omega) \simeq w_{1c} + \frac{\overline{\omega_{1c}}}{\overline{\omega^2_{1c}}} (\omega - \overline{\omega_{1c}})$.

Experimental observation of the Gaussian limit

Overbarrier passage of high-energy changed particles through a crystal in axial orientation can be essentially impact parameter independent due to the phenomenon of dynamical chaos or the crystal mosaicity. In that case, the Gaussian shape of the radiation spectrum will not be significantly affected by averaging over the beam.

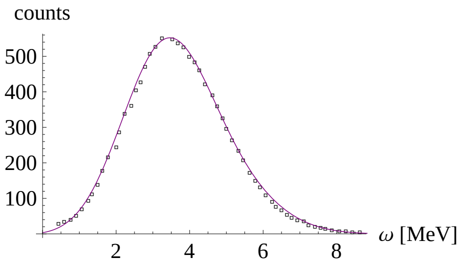

Figure: Radiation from 40 GeV electrons traversing 2.5 cm thick Ge crystal along the $\langle 110 \rangle$ axis. Points, experimental data [R. Medenwaldt et al. *Phys. Lett. B* **227** (1989) 483]. Curve, fit by Eq. (10) to the data. The inferred skewness $\gamma_3 \approx 0.02$ is small, the spectrum being almost Gaussian.

The corresponding $\bar{n}_c(\omega)$ was not measured.

Need for averaging over beam and target

The resummation procedure alone may suffice to describe observable radiation spectra, provided all the charged particles in the initial beam contribute to the spectra equivalently.
That is fulfilled for bremsstrahlung in bulk amorphous matter, coherent bremsstrahlung in crystals (for a well-collimated beam), and for undulator radiation.

But what happens for channeling radiation where different particles have different oscillation amplitudes in the channel, and therefore different radiation intensities?

Obviously, use the same resummation techniques, but average over radiation intensities *after* the resummation procedure.

The averaging procedure (positrons in harmonic channels)

For channeling of positrons, the continuous potential in the wells is approximately harmonic. Hence, the radiation intensity is $\propto E_\perp$, which is a quadratic form in $\vec{x}_0^2$, $\vec{\theta}_0^2$.

Planar channeling of a monokinetic beam ($\theta_{x0}=0$):
$\langle\ldots\rangle_{\text{beam}} = \frac{1}{2x_{0\,\max}}\int_{-x_{0\,\max}}^{x_{0\,\max}} dx_0 \ldots$.

Planar channeling of a beam with spread $\gg \theta_c$:
$\langle\ldots\rangle_{\text{beam}} = \frac{1}{E_{\perp\max}}\int_0^{E_{\perp\max}} dE_{\perp\max}\ldots$.

etc.

Generally, $\langle E_\perp\rangle_{\text{beam}} = \frac{1}{1+r}E_{\perp\max}$, where

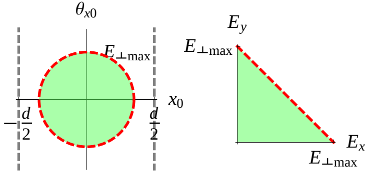

$r=2$ for planar channeling of a monokinetic beam, $r=1$ for planar channeling of a divergent beam, $r=1/2$ for axial channeling of a divergent beam, $r=0$ for fixed oscillation amplitude. Therewith, averaging of contour integral (1b) gives

$$\frac{dw_{\text{ch}}}{d\omega} = \frac{1}{2\pi i}\int_{c-i\infty}^{c+i\infty} ds e^{s\omega}\left\{F_r\left[(1+r)\int_0^\infty d\omega_1\left\langle\frac{dw_1}{d\omega_1}\right\rangle\left(1-e^{-s\omega_1}\right)\right] - F_r\left[(1+r)\langle w_1\rangle\right]\right\},$$

where $F_r(z) = \sum_{k=0}^{\infty}\frac{(-z)^k}{k!(rk+1)}$.

Salient features of channeling radiation are contained in index r.

Since F_r is a more complicated function than exponential, $\left\langle\frac{dw_1}{d\omega_1}\right\rangle$ is more difficult to reconstruct from $\frac{dw_{\text{ch}}}{d\omega}$. But in principle possible, provided $F_r(z)$ is reliably known.

Illustrations

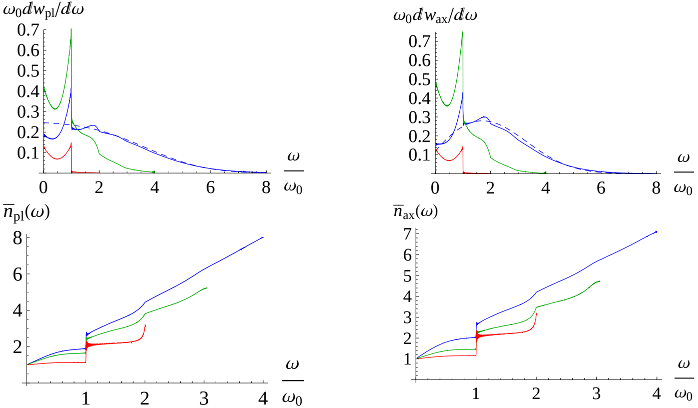

For channeling radiation (any $r > 0$), the fundamental peak does not vanish with the increase of the intensity, because a fraction of particles with moderate intensities always contributes significantly at moderate ω. Particles with high $E_\perp$ and thus high radiation intensity have Gaussian spectra, suppressed at low ω.

The axial channeling radiation case may be regarded as intermediate between planar channeling and fixed-amplitude radiation.

High-intensity limit for channeling radiation

$$\frac{dw_{\mathrm{ch}}}{d\omega} \simeq \frac{1}{2r\omega}\left[\frac{\omega}{(1+r)\left\langle\overline{\omega_{1\mathrm{c}}}\right\rangle}\right]^{\frac{1}{r}} \operatorname{erfc}\left\{\sqrt{\frac{\left\langle\overline{\omega_{1\mathrm{c}}}\right\rangle\omega}{2\left\langle\overline{\omega^2_{1\,\mathrm{c}}}\right\rangle}}\left[\ln\frac{\omega}{(1+r)\left\langle\overline{\omega_{1\mathrm{c}}}\right\rangle} + \frac{\left\langle\overline{\omega^2_{1\,\mathrm{c}}}\right\rangle}{\left\langle\overline{\omega_{1\mathrm{c}}}\right\rangle\omega}\left(\frac{1}{r}-\frac{1}{2}\right)\right]\right\} \qquad (12)$$

– broader than a Gaussian.

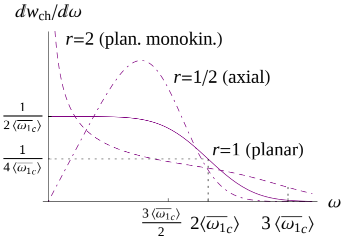

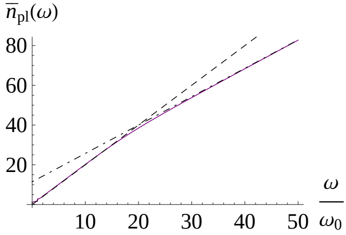

The spectrum has a break at $\omega = (1+r)\left\langle\overline{\omega_{1\,\mathrm{c}}}\right\rangle$. Below the break, there is a one-to-one correspondence between ω and $E_\perp$, and $\frac{dw_{\mathrm{ch}}}{d\omega}$ depends on ω by a power law. Beyond the break, the spectrum is determined by $E_{\perp\mathrm{max}}$, and decreases with ω exponentially.

Experiments

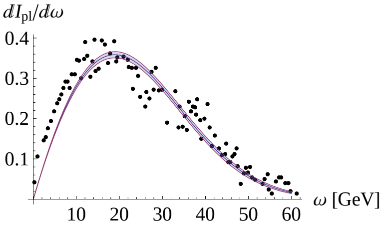

Figure: Energy spectrum of radiation from 120 GeV positrons channeling in a 2mm thick (110) Si crystal (large bending radius, $R = 11$ m). Points, experimental data [D. Lietti *et al.*, *NIM B* **283** (2012) 84]. Blue band, fit to the data by Eq. (12) with $r = 1$.

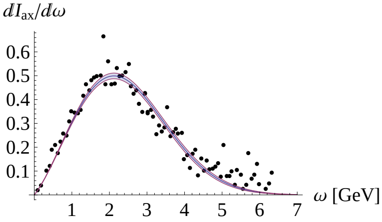

Figure: Energy spectrum of radiation from 10 GeV electrons channeling in a 3 mm thick Si crystal in orientation $\langle 111 \rangle$. Points, experimental data [M.D. Bavizhev, Yu.V. Nil'sen, and B.A. Yur'ev, *Zh. Eksp. Teor. Fiz.* **95** (1989) 1392]. Blue band, fit to the data by Eq. (12) with $r = 1/2$.

In those experiments, the radiation intensity was not very high
(the crystals only moderately thick),
but the onset of agreement with high-intensity approximations is apparent.

Pure incoherent radiation

$\frac{dw_{1i}}{d\omega_1} = \frac{a}{\omega_1}\theta(E-\omega_1)$, $\omega_1 \ll E \approx 0.5E_e$, $a \ll 1$ (semi-classical Bethe-Heitler formula).
The ensuing multiphoton spectrum

$$\frac{dw_i}{d\omega} = \frac{a}{\omega}\left(\frac{\omega}{E_e}\right)^a \frac{e^{-\gamma_E a}}{\Gamma(1+a)}. \tag{13}$$

The corresponding energy spectrum $\omega\frac{dw}{d\omega} \propto \omega^a$ mildly depends on ω, unlike the BH spectrum (see Figure).

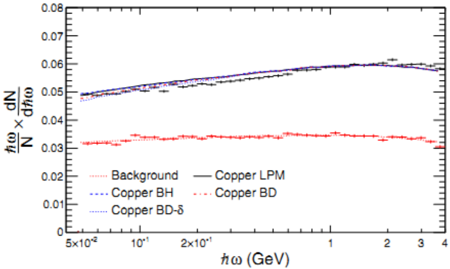

[K.K. Andersen *et al.*, *Phys. Rev. D* **88** (2013) 072007]
20 GeV electrons incident on a $2.6\%X_0$ Cu target.

$\bar{n}(\omega) = 1 + a\ln\frac{\omega}{\epsilon}$, $\omega > \epsilon$ (infrared cutoff).
so far not measured.

Mix of coherent and incoherent radiation

$$\frac{dw_1}{d\omega_1} = \frac{dw_{1c}}{d\omega_1} + \frac{dw_{1i}}{d\omega_1},$$

c – coherent radiation component,
i – incoherent radiation component,
their interference neglected.

$$\frac{dw_{1i}}{d\omega_1} = \frac{a}{\omega_1}\theta(E-\omega), \qquad a \ll 1,$$

$$\frac{dw_{1c}}{d\omega_1} = b\left(1 - 2\frac{\omega_1}{\omega_0} + 2\frac{\omega_1^2}{\omega_0^2}\right)\theta(\omega_0 - \omega_1) \qquad \text{('one-point' dipole spectrum).}$$

For analytic purposes, it is expedient to use the convolution representation:

$$\frac{dw}{d\omega} = \int_0^\omega d\omega' \frac{dw_i}{d\omega'}\frac{dw_c}{d\omega''}\bigg|_{\omega''=\omega-\omega'} + e^{-w_{1c}}\frac{dw_i}{d\omega} + \underset{\hookrightarrow 0}{e^{-w_{1i}}}\frac{dw_c}{d\omega}. \tag{14}$$

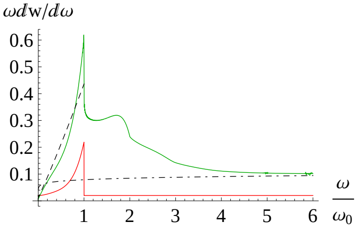

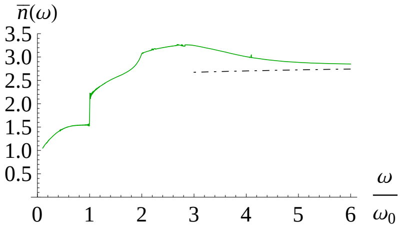

At large ω, $\bar{n}(\omega) \simeq \bar{n}_c + \bar{n}_i(\omega) = w_{1c} + 1 + a\ln\omega/\epsilon$, with ϵ an infrared cutoff.

High-intensity limit with the admixture of incoherent radiation

In the presence of an incoherent radiation component, both the mean and variance for the single-photon spectrum diverge, so the Gaussian approximation does not apply. Instead, one can use convolution representation (14) to derive [4]

$$\frac{dw}{d\omega} \approx \frac{1}{\sqrt{2\pi} E^a \overline{\omega_{1c}^2}^{\frac{1-a}{2}}} e^{-\gamma_E a - \rho^2/4} D_{-a}(-\rho), \qquad a \ll 1, \tag{15}$$

where $D_{-a}(-\rho)$ is the parabolic cylinder function.
This can be regarded as an intermediate case between Gaussian and Lévy distributions (weakly anomalous diffusion) – the tail is significant but does not dominate.

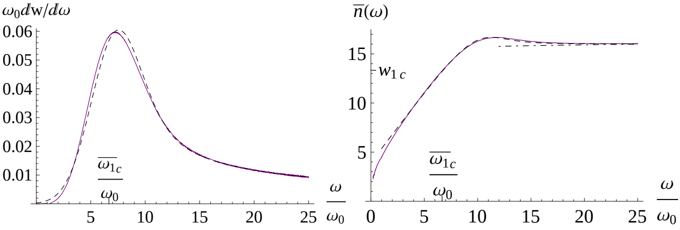

Figure: Multiphoton spectrum for $b\omega_0 = 20$, $a = 0.3$. Solid purple curve, exact distribution; dashed black curve, parabolic cylinder approximation (15).

Summary

- Resummation over multiple photon emissions is necessary for description of gamma-radiation in crystals $L \gtrsim 1$ mm thick.
- Some manifestations of multiphoton effects are likewise to those of secondary harmonics in the intra-crystal potential, non-dipole effects, or LPM-like suppression.
- At high photon multiplicity, the limiting spectrum of radiation from a prescribed current is Gaussian.
- For channeling radiation, averaging over the charged particle beam must be performed *after* the resummation. In the high-intensity limit, multiphoton channeling radiation spectra are strongly non-Gaussian. The fundamental peak survives, as well.
- With the account of incoherent radiation component, multiphoton coherent radiation spectra acquire high-ω tails, which survive in the high-intensity limit.
- Experimental studies of multiphoton effects in coherent radiation spectra were not exhaustive.

Some references

- F. Bloch and A. Nordsieck,
  Phys. Rev. **52** (1937) 54.
- L.D. Landau,
  J. Phys. USSR **8** (1944) 201.
- V.N. Baier and V.M. Katkov,
  Phys. Rev. D **59** (1999) 056003.
- M.V. Bondarenco,
  Phys. Rev. D **90** (2014) 013019.

Backup slides

Calorimeters

Narrow beaming of radiation from ultra-relativistic electrons begets a pileup problem, when different photons emitted by the same electron fly nearly along the same ray, and thus can hit the same detector cell. At practice, the objective of photon counting is commonly abandoned, and electromagnetic calorimeters are utilized for measuring only the total energy deposited by γ-quanta per electron passed through the radiator.

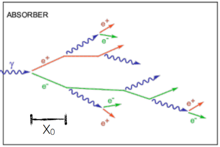

Lateral shower spread:

Main contribution must come from low energy electrons as $\langle\theta\rangle \sim 1/E_e$, i.e. for electrons with $E = E_c$ ...
Assuming the approximate range of electrons to be X_0 yields $\langle\theta\rangle \approx 21$ MeV/E_e ➛ lateral extension: $R = \langle\theta\rangle \cdot X_0$ ...

Molière Radius:

$$\boxed{R_M = \frac{21\ \mathrm{MeV}}{E_c} X_0}$$

Lateral shower spread characterized by R_M !

On average 90% of the shower energy contained in cylinder with radius R_M around shower axis ...

examples:

	X_0 (cm)	E_c (MeV)	R_M (cm)
Pb	0.56	7.4	1.6
plastic scint	34.7	80	9.1
Fe	1.76	21	1.8
Ar (liquid)	14	35	9.5
BGO	1.12	10.5	2.3
Pb glass (SF5)	2.4	11.8	4.3

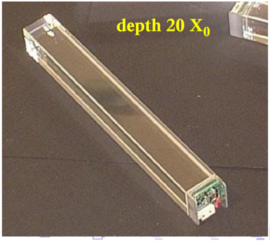

Energetically ordered form of multiphoton spectrum

Our definition was

$$\frac{dw}{d\omega} = W_0 \sum_{n=1}^{\infty} \frac{1}{n!} \int_0^{\infty} d\omega_1 \frac{dw_1}{d\omega_1} \ldots \int_0^{\infty} d\omega_n \frac{dw_1}{d\omega_n} \delta \left(\omega - \sum_{k=1}^{n} \omega_k \right). \qquad (16)$$

But since all $\omega_k > 0$,

$$\begin{aligned} \frac{dw}{d\omega} &= W_0 \sum_{n=1}^{\infty} \frac{1}{n!} \int_0^{\omega+0} d\omega_1 \frac{dw_1}{d\omega_1} \ldots \int_0^{\omega+0} d\omega_n \frac{dw_1}{d\omega_n} \delta \left(\omega - \sum_{k=1}^{n} \omega_k \right) && (17a) \\ &= e^{-\int_{\omega}^{\infty} d\omega_1 \frac{dw_1}{d\omega_1}} \frac{1}{2\pi i} \int_{c-i\infty}^{c+i\infty} ds e^{s\omega + \int_0^{\omega+0} d\omega_1 \frac{dw_1}{d\omega_1} \left(e^{-s\omega_1} - 1\right)} - W_0 \delta(\omega). && (17b) \end{aligned}$$

Eqs. (17a) compared to Eq. (16) are an *energetically ordered* form. This means that apart from the 'non-dynamical' suppressing factor

$$e^{-\int_{\omega}^{\infty} d\omega_1 \frac{dw_1}{d\omega_1}} = W_0(\omega) \qquad (18)$$

(the probability of non-emission of any photon with energy greater than ω), the multiphoton spectrum in the energetically ordered form involves only contributions from the single-photon spectrum with $\omega_1 < \omega$.